

# High Surface Area Activated Carbon from Sugar Cane Straw

Fabiana M. T. Mendes · Aline C. C. Marques ·  
Deiseane L. Mendonça · Marlucy S. Oliveira ·  
Rondinele O. Moutta · Viridiana S. Ferreira-Leitão

Received: 19 November 2014 / Accepted: 1 March 2015 / Published online: 13 March 2015  
© Springer Science+Business Media Dordrecht 2015

**Abstract** Activated carbon from sugarcane residues, bagasse and straw was obtained with phosphoric acid activation. All samples were characterized by N<sub>2</sub> adsorption–desorption isotherm, scanning electron microscopy, coupled with energy dispersive microscopy, X-ray photoelectron spectroscopy and thermal analysis. The advantages of using a ball or hammer milling process were investigated, together with the effect of the impregnation ratio and its influence on the final activated carbon porosity. The results show that all samples exhibit a high surface area and well developed porosity, but those which were ball-milled have a greater gas adsorbed amount, especially those which had straw (1415 m<sup>2</sup>/g) as precursor material. Furthermore, the results suggest that the process may have an optimum impregnation ratio, which should be around 2 or 3, respectively of the lignocellulosic source material. The mechanochemical process seems to be more relevant than the percentage of cellulose in the raw material. According with spectroscopy results, the homogeneous distribution of phosphorus throughout the sample was verified, even after

repeated washing steps. Surface phosphate linkages like C–O–PO<sub>3</sub> and C–PO<sub>3</sub> were also detected.

**Keywords** Sugarcane straw · Sugarcane bagasse · Activated carbon · Catalyst support · Ball milling process

## Introduction

The present work aims at synthesizing an active carbon from sugar cane straw with high specific surface area and mesoporous structure, envisioning its application as a catalyst support. Studies involving synthesis variables such as impregnation ratios [ $R = \text{H}_3\text{PO}_4/\text{precursor (w/w)}$ ] and the milling process will be presented here and sugarcane bagasse will be used for comparison. Sugar cane straw and bagasse were chosen for their obvious abundance as residues and the environmental benefits of their application.

In Brazil, agro industry generates around 597 million tons of residue per year [1], more especially the sugarcane sector, which represents around 25 % of the gross cultivable area in the country. Bagasse and straw are important by-products that should deserve attention as local renewable feedstock. Straw residue is becoming considerably important, especially when one takes into account the fact that it was usually burned prior to the sugarcane hand-cutting harvesting process, a practice that has recently been banned. As a matter of fact, full mechanical harvesting will result in more straw residue by 2017. A recent study [2] predicts a continuous economic growth, with an improvement of cane productivity up to 2020. Furthermore, according with Federal Law 2661 and State of São Paulo Law No. 11241 dated 19 September 2002 [3, 4]; sugarcane harvesting will have been fully converted from hand-cutting to mechanical method by the end of 2017. The switch

---

F. M. T. Mendes (✉) · A. C. C. Marques ·  
D. L. Mendonça · M. S. Oliveira · R. O. Moutta ·  
V. S. Ferreira-Leitão  
National Institute of Technology (INT), Av. Venezuela 82,  
Centro, Rio de Janeiro, RJ CEP: 20081-312, Brazil  
e-mail: fabiana.mendes@int.gov.br

### Present Address:

R. O. Moutta  
National Institute of Environment-INEA, Rua Sacadura Cabral  
103, 3° andar, sala 8, Centro, Rio de Janeiro, RJ, Brazil

V. S. Ferreira-Leitão  
Department of Biochemistry, Chemistry Institute, Federal  
University of Rio de Janeiro, Rio de Janeiro, RJ, Brazil

is being forced by the government as a way to reducing air pollution and greenhouse gas emissions. Among other various applications [1–30], including production of (2G) ethanol [6], renewable biomass has also been employed as a source of activated carbon [18–21].

Activated carbon industry and market are well established [22] where performance materials are used in multiple high-end applications. This allows its widespread use in the environmental, industrial and other sectors for removing, recovering, separating and modifying a variety of species in liquid- and gas-phase applications. The use of activated carbon in liquid media has been intensively studied by environmental scientists [23–25]. However, though not new [18], there has been renewed interest in gas-phase reactions by using it as a catalyst carrier [19, 20], especially in oxidation reactions. Charcoal (activated carbon) can be obtained from numerous biomass precursors [7–9, 17, 20], but studies dealing with sugarcane straw application are quite scarce. Besides, the need for the valuation of residues, especially those related to abundant and relatively low-value agricultural residue [18–21] such as bagasse and sugarcane straw, added to the physico-chemical characteristics of the active carbon, has motivated recent studies involving its synthesis and application in different catalytic processes [19, 20]. In this sense, properties such as a high surface area and an appropriate porosity are the most important characteristics and are the first steps towards obtaining a proper carrier. Macro and mesopores can generally be regarded as the highways into the carbon particle, and are crucial for kinetics. Most of the chemical processes make use of a catalyst and, from this point of view, a porous high surface area activated carbon can be used as support for novel catalyst (metal catalyst carriers). The internal surface is an excellent base for finely distributed active sites and provides a huge surface area for catalytic reactions. The available macropores increase the transport of reactants to and from the catalytic surface. In comparison with other carriers, activated carbon carriers have the advantage of inertness in relation to most acidic and alkaline solutions, easy recovery of precious metals, less coke production from reacting compounds (catalytic metals and the activated carbon do not form mixed compounds, and therefore do not interfere with selectivity or activity). Studies using different lignocellulosic materials [20, 26] have shown the beneficial effects of phosphorus as activation agent, coupled with its mesoporosity. In fact, resistance towards oxidation has been attributed to the presence of thermally stable phosphorus complexes that remain on the carbon surface after the activation process. The use of phosphorous activated carbon is especially interesting when one has in mind its future use in the oxidation reaction, also because of its thermal stability [20].

## Materials and Methods

Sugarcane straw is an important and abundant residue. In this section we will describe the methodology to prepare an activate carbon from straw by using phosphorous as an activation agent. Moreover, two types of mechanical milling process (hammer and ball mill) were used. Reports by using different lignocellulosic materials [20, 26] have shown the beneficial effects of phosphorus as an activation agent, coupled with its mesoporosity. The use of phosphorous activated carbon is especially interesting when one has in mind its future use in the oxidation reaction, also because its thermal stability [20].

### Preparation of Activated Carbon

Straw from sugar cane, supplied by Complexo Bioenergético Itarumã S.A, Goiás, Brasil, was used as a starting material for obtaining high surface area activated carbons. The lignocellulosic source has the following chemical composition (average values) [5]: cellulose (29.3 %), hemicellulose (30.3 %), soluble lignin (9.7 %), insoluble lignin (20.2 %), extractives (10.7 %) and ashes (2.7 %).

The straw was processed in a hammer-mill and sieved, which resulted in fractions around 2 mm. Another milling process was performed using a ball mill in order to reduce the particle size and to investigate the mechanical influence on the final activated carbon porosity. The ball milling process generates fractions around 1 mm.

For the impregnating and activating processes, the same procedure was used for both straw's particle sizes. The precursor was impregnated with 85 % (w/w)  $H_3PO_4$  (Sigma Aldrich) aqueous solution at room temperature for 2 h, and dried in a rotary evaporator for 24 h, at 60 °C. Two impregnation ratios were used [ $R = H_3PO_4$ /precursor (w/w)]: named SBM2 and SBM3 (“*Straw Ball Milled*”), for  $R = 2$  and 3, respectively. The one named SHM9 (“*Hammer-Milled Straw*”) refers to the hammer-milled straw with a ratio of 9. The obtained materials were kept in an oven at 100 °C for 72 h. After drying, the impregnated straws were activated at 500 °C, under continuous  $N_2$  flow (60 mL/min), in a conventional tubular reactor. The activation temperature was reached at a heating rate of 10 °C/min and maintained for 2 h.

The activated samples were cooled in  $N_2$  flow. After that, the samples were washed and filtered with distilled hot water (60 °C) until neutral pH. The resulting activated charcoal was dried at 100 °C for 24 h and stocked, prior to characterization analysis.

The same experiment was also carried out with bagasse as raw material, which was supplied by Cooperativa Agroindustrial do Rio de Janeiro Ltda (COAGRO, RJ). Bagasse was milled sequentially, first in a hammer mill and

then in a ball mill (BBM3). This sample was prepared with ratio equal to  $R = 3$ .

### Characterization

Characterization Technics such as  $N_2$  adsorption–desorption (BET), X-ray photoelectron spectroscopy (XPS), infrared spectroscopy (FTIR) and scanning electron spectroscopy coupled with energy dispersion spectroscopy (EDS) were used to characterize the prepared samples. In this section we present the experimental details of each technique. The obtained results will be presented and discussed in the “[Results and Discussion](#)” Section. Properties such as a high surface area and an appropriate porosity are the most important characteristics and are the first steps towards obtaining a proper catalyst carrier. Macro and mesopores can generally be regarded as the highways into the carbon particle, and are crucial for kinetics.

### $N_2$ Adsorption–Desorption

The porous structure of the activated carbons was characterized by  $N_2$  adsorption–desorption at  $-196\text{ }^\circ\text{C}$  and performed with ASAP 2020 equipment (Micromeritics). Samples were pretreated in vacuum at a temperature of  $300\text{ }^\circ\text{C}$  for 24 h. From the  $N_2$  isotherm, the specific surface area ( $S_{\text{BET}}$ ) was obtained by the Brunauer–Emmert–Teller (BET) method, total pore volume ( $V_{\text{total}}$ ) and average pore diameter ( $D_p$ ) by Barrett–Joyner–Halenda (BJH) method and external area ( $S_t$ ) and micropore volume ( $V_{\text{meso}}$ ) by t-plot method. Micropore area ( $S_{\text{meso}}$ ) corresponds to the difference between surface area ( $S_{\text{BET}}$ ) and external area ( $S_t$ ).

### X-Ray Photoelectron Spectroscopy (XPS)

The surface chemistry of samples was analyzed by X-ray photoelectron spectroscopy (XPS). Analyzes were performed using a hemispherical spectrometer PHOIBOS 150—SPECS, equipped with X-ray Gun (XR-50) with Al  $K\alpha$  source (1486.6 eV), which is non-monochromatic. The binding energy shifts due to surface charging were corrected using the C 1s level at 284.6 eV, as an internal standard. Spectra were Shirley background-subtracted across the energy region and fitted using CasaXPS Version 2.3.15. The base pressure in the analysis chamber was kept in the range  $5 \times 10^{-10}$ – $1 \times 10^{-9}$  mbar.

### Scanning Electron Microscopy (MEV-EDS)

The surface texture of the samples was characterized by scanning electron microscopy (SEM) and the distribution of the phosphorous was determined by energy dispersive

spectroscopy (EDS) analyses. Both were obtained using SEM–EDS—Inspect S50, FEI.

Non-isothermal thermogravimetric analyses were carried out in a gravimetric thermobalance system, SDT Q600 Dp union. The thermobalance automatically measures the weight and temperature as a function of time. Experiments were carried out in air atmosphere with the use of a sample mass of approximately 10 mg. The sample was increased from room temperature up  $500\text{ }^\circ\text{C}$ .

### Infrared Spectroscopy (FTIR)

FTIR-IR spectrum of the SBM3 sample (85 mg) was obtained using a spectrometer Magma-IR560 spectrometer at room temperature by the KBr method (500:1). The nature of the surface groups was evaluated.

## Results and Discussion

This section presents some of the most relevant aspects pertaining to the physical–chemical characterization of straw and active carbon. The results reveal that a high specific surface area ( $1415\text{ m}^2/\text{g}$ ) activated carbon can be obtained, while using a ball milling process and a phosphorous activating process.

Sugar cane straw and bagasse were previously used by our group [5], whose chemical composition is reproduced in Table 1 [5].

As we are dealing with a lignocellulosic biomass, it is more relevant to establish its composition in terms of its cellulose, hemicellulose and lignin amounts. In this way, one can distinguish among amorphous and crystalline fractions. There are indicative studies showing that the phosphorous linkages are preferentially formed in the crystalline part, providing resistance and porosity [9].

The residual amounts of inorganic elements of the prepared activated carbon from straw were estimated by EDS technique and revealed relative weight% amounts of 0.1 % (Al), 2.8 % (Si) and 12.2 % (P).

Figure 1 shows the  $N_2$  adsorption–desorption isotherm at  $-196\text{ }^\circ\text{C}$  from the SHM9 sample and presents a

**Table 1** Chemical composition of sugarcane bagasse and straw used as raw materials to obtain activated carbon

Components% (w/w)	Bagasse (%)	Straw (%)
Cellulose	$36.58 \pm 0.73$	$29.25 \pm 1.08$
Hemicellulose	$22.96 \pm 2.93$	$30.34 \pm 3.43$
Lignin	$27.34 \pm 0.24$	$29.90 \pm 0.28$
Ashes	$6.89 \pm 0.01$	$2.67 \pm 0.14$
Extractives	$5.62 \pm 0.37$	$8.41 \pm 2.15$

modified type II isotherm with hysteresis loop starting at relative pressures near 0.7, suggesting a broad pore size distribution. In fact, it is well known that activated carbons contain micro, meso and macropores in its structure, but the relative ratio varies considerably, depending on the precursor and the manufacturing process used. The profiles of isotherms of SBM2, SBM3 and BBM3 samples are shown in Fig. 2. They are also modified type II isotherm, however with hysteresis loops at relative pressures near 0.4, which indicates a significantly higher contribution of micro and mesoporosity. Notwithstanding this, it is possible to realize that ball-milled samples have a greater amount of absorbed gas, especially those which had straw as precursor material (sample SBM2).

As proposed by Rosas et al. [7, 9, 26] activation with phosphoric acid resulted in significant pore development with a high contribution from mesopores, interacting with lignocellulosic material to form phosphate and polyphosphate bridges.

According to this literature, these bridges connect biopolymer fragments and promote an expansion of the carbonaceous matrix, which suggests that the phosphate groups are responsible for developing the porosity. The impregnation ratio (weight of  $H_3PO_4$  in solution/weight of source) was pointed out by these authors as of some importance in the mesoporosity creation mechanism. On the other hand, Chen et al. [8] have shown that the employment of a mechanochemical process can also contribute to development of mesoporosity. These authors highlighted the advantages of using a ball milling process, such as less processing time, greater adsorption capacity and higher adsorption volume of nitrogen. Therefore, in the present paper, we intentionally worked with an extremely high impregnation ratio (SHM9) and also made use of the ball milling process, however with impregnation ratios at a

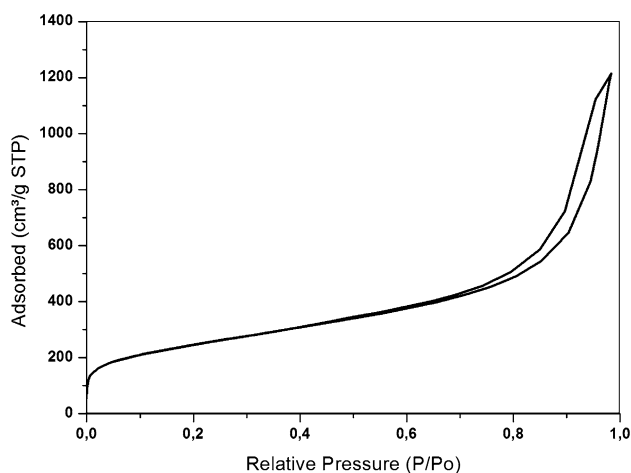


**Fig. 1**  $N_2$  adsorption–desorption isotherm at  $-196\text{ }^\circ\text{C}$  from the SHM9 sample

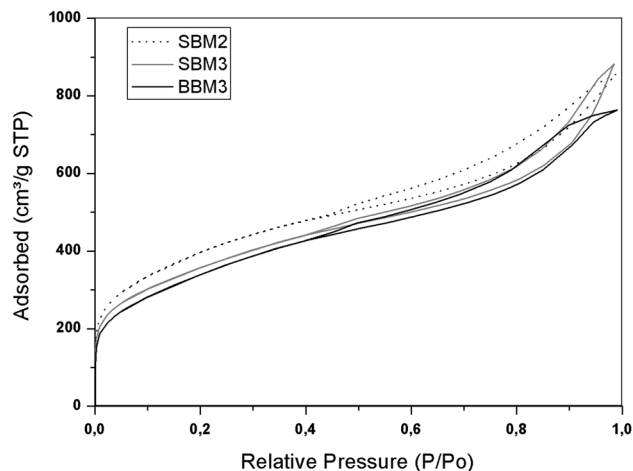


**Fig. 2**  $N_2$  adsorption–desorption isotherm at  $-196\text{ }^\circ\text{C}$  from the SBM2, SBM3 and BBM samples

similar range (2 and 3) as used before [7–9, 20]. Notwithstanding this, we need always to bear in mind that sugarcane straw is being used as raw material, unlike the previously reported research. With the help of calculated textural parameters of prepared samples (Table 2), it is possible to see the effect of impregnation ratio and the milling process. All samples present developed mesoporosity, but the one that was prepared with a higher impregnation ratio (SHM9) exhibits lower BET surface, a broader pore size distribution and lower micropore volume. These results suggest that there may be an optimum impregnation ratio during the preparation process, which should be around 2 or 3, irrespectively of the lignocellulosic source material used. Apart from that, a narrow pore size distribution, with a 33–51 Å range (SBM2) can be obtained when using impregnation ratios of 2 or 3, which also results in higher surface areas (see Fig. 4). Rosas et al. [9] also observe a tendency of larger pore size formation with an increase of impregnation ratio.

The  $S_{BET}$  to SBM2, SBM3 and BBM3, all milled in a ball mill, are very similar and higher than SHM9 sample. These results show the advantage of the use of a mechanochemical process, in agreement to what has been proposed by Chen et al. [8].

As mentioned before, t-plot method was generally used to determine  $S_t$  and  $V_{micro}$  and the most popular thickness equation is the Harkins–Jura equation. However, as proposed by the ASTM standardization [28], the Eq. 1 (ASTM standard D-6556-01) would be more suitable to employ when carbon-like materials are being analyzed. The Eq. 1, the so-called carbon black equation, was used in the present work, but the calculated results were quite similar to the ones obtained when using Harkins–Jura equation. The t-plot graphic is shown in Fig. 3.

**Table 2** Texture properties of prepared activated carbon samples

Sample	$S_{\text{BET}}^{\text{a}}$ (m <sup>2</sup> /g)	$S_{\text{meso}}^{\text{a}}$ (m <sup>2</sup> /g)	$S_{\text{micro}}^{\text{b}}$ (m <sup>2</sup> /g)	$V_{\text{micro}}^{\text{a}}$ (cm <sup>3</sup> /g)	$V_{\text{meso}}^{\text{a}}$ (cm <sup>3</sup> /g)	$D_{\text{p}}^{\text{a}}$ (Å)
Straw—hammer mill (SHM9)	875	683	192	0.09	19.34	78.63
Straw—ball mill (SBM2)	1415	894	521	0.24	15.02	37.08
Straw—ball mill (SBM3)	1279	819	460	0.21	13.53	45.52
Bagasse—ball mill (SBB3)	1236	853	383	0.17	13.06	34.24

<sup>a</sup>  $S_{\text{BET}}$  refer to BET surface area,  $S_{\text{meso}}$  refer to mesopore area,  $S_{\text{micro}}$  refer to micropore area,  $V_{\text{mp}}$  refer to micropore volume,  $V_{\text{meso}}$  refer to mesopore volume and  $D_{\text{p}}$  refer to average pore diameter

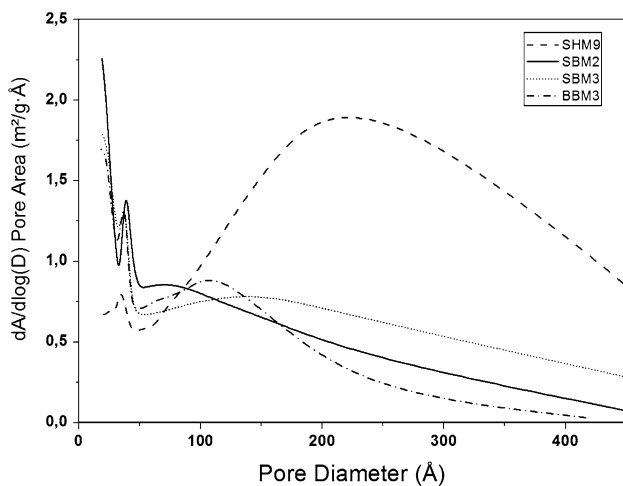
<sup>b</sup> Correspond to the difference between surface area ( $S_{\text{BET}}$ ) and external area ( $S_{\text{t}}$ )

$$t = 0.88(P/P_0)^2 + 6.45(P/P_0) + 2.98 \quad (1)$$

Pore size distribution of an activated carbon sample is one of the most important parameters because it controls the diffusion of reactants and products in/out the catalyst structure. Micropores and mesopores also contribute to the adsorption capacity of the activated carbon, while macropores act as a transport way in order for the molecules to reach other types of pores. In conclusion, ball-milled samples presented better results, as shown in Table 2 and Fig. 3.

Rosas et al. [7, 9] evaluated the porosity of activated carbons with hemp fibers and monoliths from hemp cane as precursors. It is suggested that the hemp fibers have more potential for dilation because it contains significantly higher amounts of cellulose than hemicellulose and lignin. According to the study, the presence of cellulose induces the formation of mesopores. In this work, the influence of the cellulose percentage present in the raw material is not significant as compared to the effect of the mechanochemical process.

Figure 4a, b shows SEM micrographs of straw *in nature* and activated carbon (SHM sample). Figure 4a shows the

**Fig. 3** Pore size distributions of SHM, SBM and BBM samples

straw as received and as expected. Moreover, it exhibits the uniform and fibrous structure of the untreated raw material as described by Moutta et al. [5]. Figure 4b illustrates the structure of the activated carbon, which allows the identification of morphological differences, once the activated carbon no longer shows the previously well-defined structure as in the untreated straw. This demonstrates the complete disruption of the material structure. The energy dispersive spectroscopy (EDS) analysis reveals an homogeneous phosphorous distribution throughout the studied area. The semi-quantitative analysis indicates that a value of about 12 % (weight%) of phosphorous is present, which demonstrates that phosphorous still remains, even after repeated washing. The presence of inorganic elements, such as Al (0.1 % weight) and Si (2.8 % weight) were also verified.

The results of thermogravimetric analysis of SBM and BBM samples are shown in Fig. 5. As can be seen, activated carbon is resistant in air up to 750 °C. Above this temperature, the material is completely degraded. The profile of the weight-loss curve is very similar for all samples. At temperatures lower than 350 °C, samples exhibit a small weight loss that can be attributed to the release of moisture. The abrupt weight loss at temperatures between 200 and 500 °C can be related to decomposition of major biopolymers and, at temperatures higher than 500 °C, to a deeper degradation of the more stable volatile matter. As can be seen, impregnation with phosphoric acid gives a higher thermal resistance to the prepared materials.

There are few papers presenting XPS surface chemistry characterization of activated carbons from lignocellulosic materials [7, 9, 19], but not of an activated carbon obtained from sugarcane straw. The surface chemistry composition of sample SBM3 was investigated by XPS analysis. As expected for the other lignocellulosic materials, the survey spectrum revealed the presence of carbon (C), oxygen (O) and phosphorous (P). The presence of fluorine (F) and silicon (Si) was also detected. The presence of phosphorus (about 7 % atomic percent) on the surface could be verified, even after successive washes to remove excessive



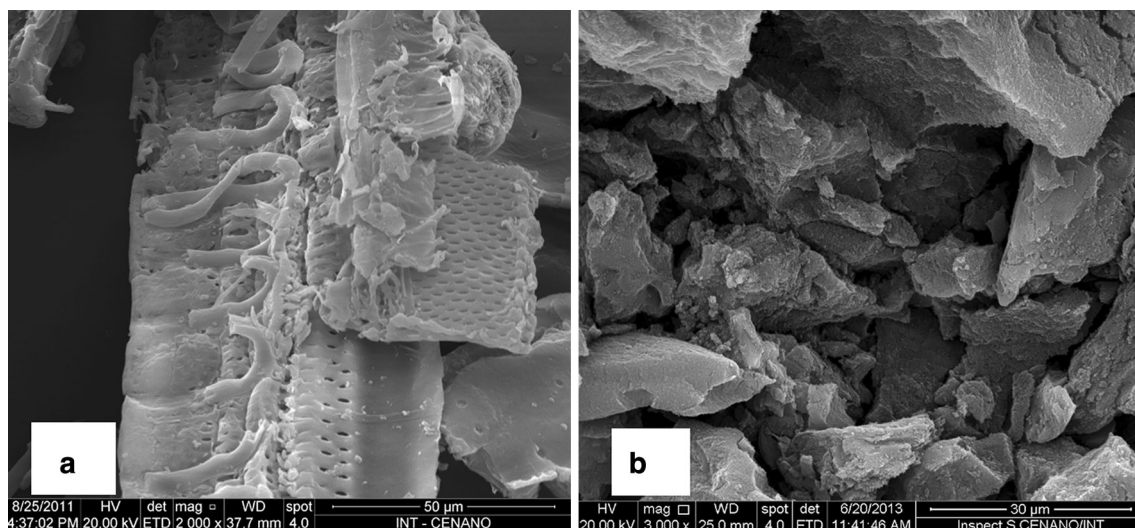


**Fig. 4** SEM micrographs of raw material-sugarcane straw (a) and sugarcane straw-derived activated carbon: SHM (b)

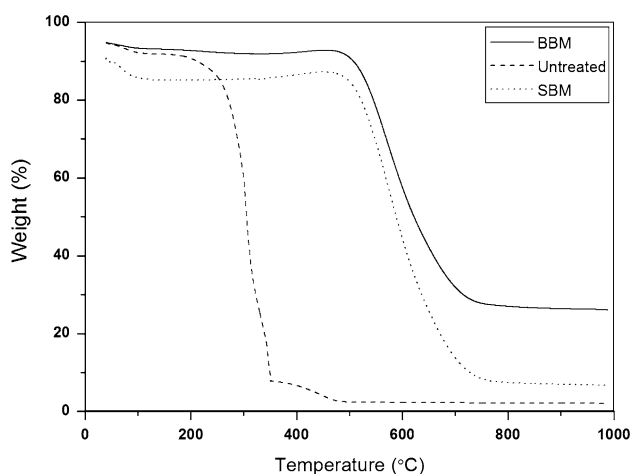


**Fig. 5** Thermogravimetric analysis in air atmosphere for sugarcane bagasse and straw treated and untreated with phosphoric acid

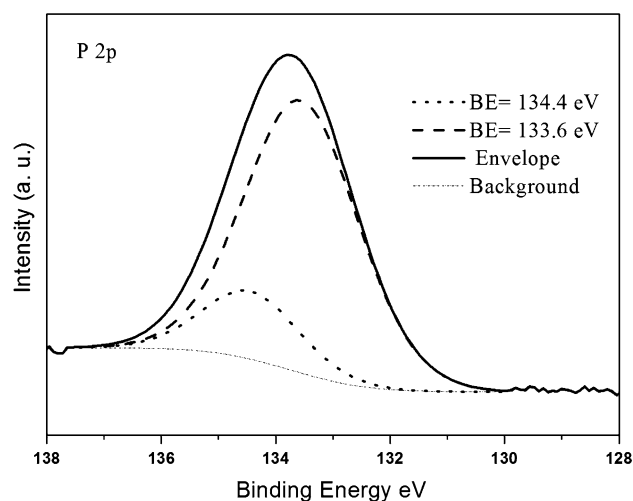


**Fig. 6** Photoelectron P<sub>2p</sub> spectrum of sample SBM3

acid and ash. The high resolution P<sub>2p</sub> spectrum for the activated carbon (SBM3 sample) is presented in Fig. 6. The P<sub>2p</sub> spectrum of phosphorus shows contribution of two peaks at binding energies of 134.4 and 133.6 eV. Like the activated carbon obtained from other lignocellulosic materials, the high energy peak could be related to the presence of C–O–PO<sub>3</sub>, while the one at a lower binding energy to C–PO<sub>3</sub> groups. Rosas et al. [26] made a comparative study of the oxidation kinetics of the chars and activated carbons of different biomass residues (lignin, hemp stem and olive stone). They concluded that the activation with phosphoric acid really produces activated carbons with oxidation resistance, which can be attributed to the phosphorus groups present on the surface. They show that these groups are produced during the preparation process and remain stable even after the surface washing process. They

suggest that the phosphorus groups, mainly C–O–PO<sub>3</sub>, act as inhibitors of carbon gasification, because they stabilize the carbon active sites and act as a physical barrier to oxygen. Guerrero-Pérez et al. [20] while working with orange skin as an activated carbon source, have also observed surface groups such as COP<sub>3</sub>, C<sub>3</sub>P and CPO<sub>3</sub>. These groups are formed and stabilized on the surface conferring resistance towards oxidation, an important property when one plans to employ water in the reaction medium, as is the case of oxidation reactions [20, 29]. It is generally accepted that phosphoric acid acts both by forming phosphate linkages and broadening porous structures in activated carbons. The present work shows that activated carbon prepared from sugarcane straw has a similar behavior while forming phosphate linkages and that it can be used as an auspicious support for metal to catalyze oxidation reaction and others.

As expected, FTIR of prepared SBM3 sample result show a typical spectrum [30] and reveals a wide transmission band at 3200–3600  $\text{cm}^{-1}$ . This band can be assigned to the O–H stretching mode of hydroxyl groups and adsorbed water. The weak bands around 2900 and 2859  $\text{cm}^{-1}$  can be assigned to aliphatic, C–H stretching in  $-\text{CH}_2-$ . The weak band observed at 1451  $\text{cm}^{-1}$  can be related to  $-\text{CH}_2-$  deformation. The presence of this last band suggests a low oxidized surface. The contributions of Aromatic structures vibration are irrelevant.

## Conclusion

The main conclusion that can be drawn from this work is that a high surface area (1415  $\text{m}^2/\text{g}$ ) activated carbon from sugarcane residues, especially sugarcane straw, can be obtained. In this work, the creation of such high surface area was favored by the use of a ball milling process before the chemical activation with phosphoric acid. Surface properties of these activated carbon materials were significantly influenced by the impregnation ratio and by the milling process as well. The ball milling process is particularly advantageous, once it helps developing a narrower mesopore size distribution. The use of an extremely high impregnation ratio gives a broad range of mesopore size distribution, which suggests that there is an optimum impregnation ratio. Such ratio should be around 2 or 3, which results in a narrower mesopore distribution. The presence of phosphorus is homogeneously distributed throughout the sample, even after repeated washing steps. The presence of surface phosphorous like C–O– $\text{PO}_3$  and C– $\text{PO}_3$  was also detected on the surface of the activated carbon prepared from sugarcane residues. This promising material will be further used as a catalyst support towards oxidation reactions.

**Acknowledgments** We acknowledge the financial support from Brazilian funding agency FAPERJ-APQ-1/2013-1 Proc. No. 111.405/2013, to the CIEE and Sisnano program.

## References

1. Ferreira-Leitão, V.S., Gottschalk, L.M.F., Ferrara, M.A., Nepomuceno, A.L., Molinari, H.B.C., Bon, E.P.S.: Biomass residues in Brazil: availability and potential uses. *Waste Biomass Valor* **1**, 65–76 (2010)
2. Ferreira Filho, J.B.S., Horridge, M.: Ethanol expansion and indirect land use change in Brazil. *Land Use Policy* **36**, 595–604 (2014)
3. Brazilian Federal Law: Decreto no. 2.661, 8th of July of 1998. [http://www.planalto.gov.br/ccivil\\_03/decreto/D2661.htm](http://www.planalto.gov.br/ccivil_03/decreto/D2661.htm)
4. Brazilian State of São Paulo Law: Lei no. 11.241/02. <http://governo-sp.jusbrasil.com.br/legislacao/94008/lei-11241-02>
5. Moutta, R.O., Silva, M.C., Corrales, R.C.N.R., Cerullo, M.A.S., Ferreira-Leitão, V.S., Bon, E.P.S.: Comparative response and structural characterization of sugarcane bagasse, straw and bagasse-straw 1:1 mixtures subjected to hydrothermal pretreatment and enzymatic conversion. *J. Microbial Biochem. Technol.* **S12**, 1–8 (2013)
6. Corrales, R.C.N.R., Mendes, F.M.T., Perrone, C.C., Sant'Anna, C., Sousa, W., Abud, Y., et al.: Structural evaluation of sugar cane bagasse steam pretreated in the presence of  $\text{CO}_2$  and  $\text{SO}_2$ . *Biotechnol. Biofuels* **5**, 36 (2012)
7. Rosas, J.M., Bedia, J., Rodríguez-Mirasol, J., Cordero, T.: Preparation of hemp-derived activated carbon monoliths: adsorption of water vapor. *Ind. Eng. Chem. Res.* **47**, 1288–1296 (2008)
8. Chen, C.X., Huang, B., Li, T., Wu, G.F.: Preparation of phosphoric acid activated carbon from sugarcane bagasse by mechanochemical processing. *BioResources* **7**(4), 5109–5116 (2012)
9. Rosas, J.M., Bedia, J., Rodríguez-Mirasol, J., Cordero, T.: HEMP-derived activated carbon fibers by chemical activation with phosphoric acid. *Fuel* **88**, 19–26 (2009)
10. Castro, J.B., Bonelli, P.R., Cerrella, E.G., Cukierman, A.L.: Phosphoric acid activation of agricultural residues and bagasse from sugar cane: influence of the experimental conditions on adsorption characteristics of activated carbons. *Ind. Eng. Chem. Res.* **39**, 4166–4172 (2000)
11. Devnarain, P.B., Arnold, D.R., Davis, S.B.: Production of activated carbon from south African sugarcane bagasse. *Proc. S. Afr. Sug. Technol. Ass.* **76**, 477–489 (2002)
12. Wu, X., Radovic, L.R.: Inhibition of catalytic oxidation of carbon/carbon composites by phosphorus. *Carbon* **44**, 141–151 (2006)
13. Qureshi, K., Bhatti, I., Kazi, R., Ansari, A.K.: Physical and chemical analysis of activated carbon prepared from sugarcane bagasse and use for sugar decolorisation. *Int. J. Chem. Bio. Eng.* **1**, 145–149 (2008)
14. Demiral, I., Demiral, H.: Surface characterization of activated carbons obtained from olive bagasse by chemical activation. *Surf. Interface Anal.* **42**, 1347–1350 (2010)
15. Carvalho, J., Araujo, J., Castro, F.: Alternative low-cost adsorbent for water and wastewater decontamination derived from eggshell waste: an overview. *Waste Biomass Valor* **2**, 157–167 (2011)
16. Pippo, W.A., Luengo, C.A., Alberteris, L.A.M., Garzone, P., Cornacchia, G.: Energy recovery from sugarcane-trash in the light of 2nd generation biofuels. Part 1: Current situation and environmental aspects. *Waste Biomass Valor* **2**, 1–16 (2011)
17. Altendor, S., Neibi, M.C., Brehm, N., Emmanuel, E., Gaspard, S.: Pilot-scale synthesis of activated carbons from vetiver roots and sugar cane bagasse. *Waste Biomass Valor* **4**, 485–495 (2013)
18. Brinen, J.S., Schmitt, J.L., Doughman, W.R., Achorn, P.J., Siegel, L.A.: X-ray photoelectron spectroscopy studies of the rhodium on charcoal catalyst. *J. Catal.* **40**, 295–300 (1975)
19. Pande, G., Selvakumar, S., Batra, V.S., Gardoll, O., Lamonier, J.F.: Unburned carbon from bagasse fly ash as a support for a VOC oxidation catalyst. *Catal. Today* **190**, 47–53 (2012)
20. Guerrero-Pérez, M.O., Rosas, J.M., López-Medina, R., Bañares, M.A., Rodríguez-Mirasol, J., Cordero, T.: Lignocellulosic-derived catalysts for the selective oxidation of propane. *Catal. Commun.* **12**, 989–992 (2011)
21. Clark, J., Macquarrie, D., Gronnow, M., Budarin, V.: Green chemistry principles. In: Boodhoo, K., Harvey, A. (eds.) *Process intensification for green chemistry*, vol. 1, pp. 35–55. Noida, India (2013)
22. Scheffer, K.: Activated carbon 2014 Market update or...the Carbon Cosmos. Spotlight. *Water Conditioning and Purification*.

- Features, 30–32, 06 June 2014. [www.wcponline.com/pdf/June\\_2014\\_Schaeffer.pdf](http://www.wcponline.com/pdf/June_2014_Schaeffer.pdf) (2014)
23. Gupta, V.K., Ali, I., Saini, V.K., Van Gerven, T., Van der Bruggen, B., Vandecasteele, C.: Removal of dyes from wastewater using bottom ash. *Ind. Eng. Chem. Res.* **44**(11), 3655–3664 (2005)
  24. Gupta, V.K., Ali, I.: Removal of DDD and DDE from wastewater using bagasse fly ash, a sugar industry waste. *Water Res.* **35**(1), 33–40 (2001)
  25. Mittal, A., Mittal, J., Malviya, A., Kaur, D., Gupta, V.K.: Decoloration treatment of a hazardous triarylmethane dye, Light Green SF (Yellowish) by waste material adsorbents. *J. Colloid Interface Sci.* **342**, 518–527 (2010)
  26. Rosas, J.M., Ruiz-Rosas, R., Rodríguez-Mirasol, J., Cordero, T.: Kinetic study of the oxidation resistance of phosphorus-containing activated carbons. *Carbon* **50**, 1523–1537 (2012)
  27. Haber, J.: International Union of Pure and Applied Chemistry. Manual on catalyst characterization (Recommendations 1991). *Pure Appl. Chem.* **63**, 1227–1246 (1991)
  28. ASTM International. Standard test method for carbon black—total and external area by nitrogen adsorption. Designation D6556-10
  29. Sun, M., Zhang, J., Putaj, P., Caps, V., Lefebvre, F., Pelletier, J., Basset, J.M.: Catalytic oxidation of light alkanes (C<sub>1</sub>–C<sub>4</sub>) by heteropoly compounds. *Chem. Rev.* **114**, 981–1019 (2014)
  30. Puziy, A.M., Poddubnaya, O.I., Martínez-Alonso, A., Suárez-García, F., Tascón, J.M.D.: Synthetic carbons activated with phosphoric acid III. Carbons prepared in air. *Carbon* **41**, 1181–1191 (2003)